

25. MAJOR AND TRACE ELEMENTS AND Nd AND Sr ISOTOPE GEOCHEMISTRY OF BASALTS FROM THE DEEP SEA DRILLING PROJECT LEG 74 WALVIS RIDGE TRANSECT¹

S. H. Richardson, Center for Geochemistry, Department of Earth and Planetary Sciences, Massachusetts Institute of Technology, Cambridge, Massachusetts

and

A. J. Erlank, D. L. Reid, and A. R. Duncan, Department of Geochemistry, University of Cape Town, Rondebosch 7700, Republic of South Africa

ABSTRACT

Basement intersected in Holes 525A, 528, and 527 on the Walvis Ridge consists of submarine basalt flows and pillows with minor intercalated sediments. These holes are situated on the crest and mid- and lower NW flank of a NNW-SSE-trending ridge block which would have closely paralleled the paleo mid-ocean ridge. The basalts were erupted approximately 70 Ma, a date consistent with formation at the paleo mid-ocean ridge. The basalt types vary from aphyric quartz tholeiites on the Ridge crest to highly plagioclase phyric olivine tholeiites on the flank. These show systematic differences in incompatible trace element and isotopic composition, and many element and isotope ratio pairs form systematic trends with the Ridge crest basalts at one end and the highly phyric Ridge flank basalts at the other.

The low $^{143}\text{Nd}/^{144}\text{Nd}$ (0.51238) and high $^{87}\text{Sr}/^{86}\text{Sr}$ (0.70512) ratios of the Ridge crest basalts suggest derivation from an old Nd/Sm and Rb/Sr enriched mantle source. This isotopic signature is similar to that of alkaline basalts on Tristan da Cunha but offset by somewhat lower $^{143}\text{Nd}/^{144}\text{Nd}$ values. The isotopic ratio trends may be extrapolated beyond the Ridge flank basalts (which have $^{143}\text{Nd}/^{144}\text{Nd}$ of 0.51270 and $^{87}\text{Sr}/^{86}\text{Sr}$ of 0.70417) in the direction of typical MORB compositions. These isotopic correlations are equally consistent with mixing of depleted and enriched end-member melts or partial melting of an inhomogeneous, variably enriched mantle source. However, observed Zr-Ba-Nb-Y interelement relationships are inconsistent with any simple two-component model of magma mixing or partial melting. They also preclude extensive involvement of depleted (N-type) MORB material or its mantle sources in the petrogenesis of Walvis Ridge basalts.

INTRODUCTION

Ever since Wilson (1963) proposed that the Walvis Ridge might represent a mantle plume trace it has been suspected that this feature was igneous in origin. Basalts with alkaline affinities were subsequently dredged from the vicinity of the Ridge (Hekinian, 1972; Humphris and Thompson, 1981). This served to strengthen the association with the volcanic islands of Tristan da Cunha and Gough, which lie on an approximate SW extension of the Ridge. Among the range of models advanced for the formation of this and other aseismic ridges (Dingle and Simpson, 1976), the hotspot or mantle plume hypothesis stands out as having attracted the most support (Morgan, 1971, 1972; Goslin and Sibuet, 1975; Burke and Wilson, 1976; Detrick and Watts, 1979). Until recently, however, an oceanic crustal origin for the Walvis Ridge could not be presumed, given the divergence between its overall orientation and adjacent crustal flow lines. In an alternative proposal (van der Linden, 1980) the Ridge originated as a fragment of continental crust which split from the main continental mass during early rifting of the South Atlantic.

On the basis of detailed bathymetry and magnetic anomaly identification (Rabinowitz and LaBrecque, 1979; Rabinowitz and Simpson, 1979), Rabinowitz (this

volume) has suggested that NNW-SSE-oriented segments of the Walvis Ridge originated at the paleo mid-ocean ridge, followed by successive ridge jumps. On Leg 74, Walvis Ridge transect basement rocks in the form of tholeiitic basalt flows and pillows were recovered by drilling. The geochemical character of these rocks is obviously pertinent to any scheme for their petrogenesis at a mid-ocean ridge. Their deviant trace element and Nd and Sr isotope geochemistry relative to average mid-ocean ridge basalts (MORB), detailed below, provides direct evidence for the presence of chemically modified mantle beneath the Ridge, previously suggested by Chave (1979) on the basis of regional Rayleigh wave dispersion characteristics.

GEOLOGICAL SETTING AND SAMPLING

Walvis Ridge basement was encountered at Leg 74 Sites 525, 528, and 527, respectively situated on the crest and mid- and lower NW flank of the Ridge (see site chapters, this volume). The transect was located on a NNW-trending block which would have closely paralleled the paleo-ridge axis. At all three sites the basement complex consists of basalt flows with thin, glassy upper chilled margins and minor intercalated volcanoclastic and biogenic sediments (Fig. 1). Glassy margins, grain-size variation, macroscopic petrography, and sediment breaks serve to define the cooling units enumerated in Figure 1. A distinctive pillow basalt sequence occurring in the crestal Hole 525A confirms the submarine extrusive ori-

¹ Moore, T. C., Jr., Rabinowitz, P. D., et al., *Init. Repts. DSDP, 74*: Washington (U.S. Govt. Printing Office).

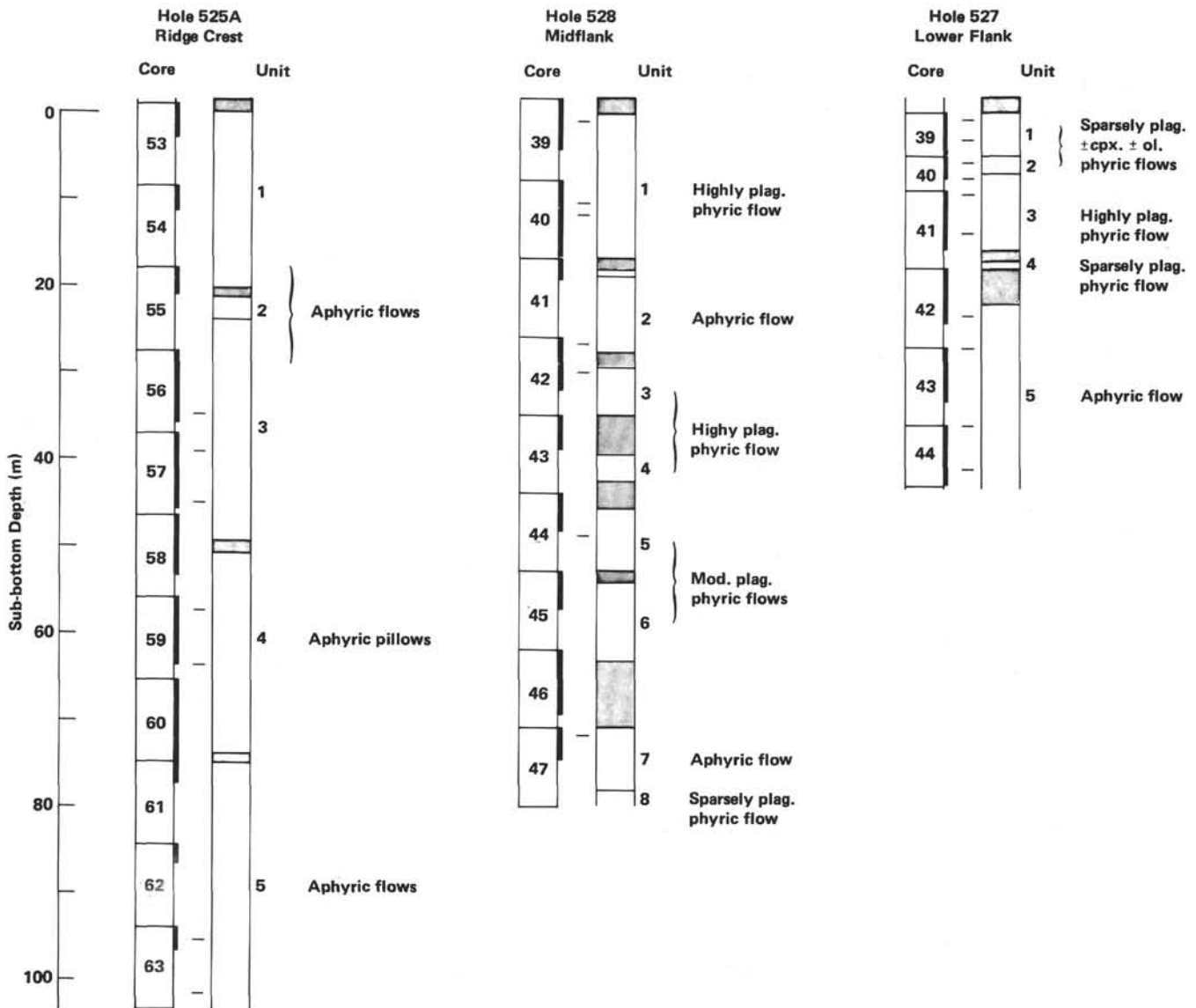


Figure 1. Schematic representation of basalt lithology in Leg 74 Holes 525A, 528, and 527, respectively situated on the crest, midflank, and lower flank of the Walvis ridge. Sub-bottom depth is the same scale for all three holes. Solid vertical bars = recovery, dashes = sample locations, and shading = intercalated sediment horizons.

gin of the Ridge volcanics. On the basis of both magnetostratigraphy (Magnetic Anomaly 31 to 32 time) and biostratigraphy of intercalated and overlying sediments (Maestrichtian to Campanian time), basement rocks in this segment of the Ridge are thought to be approximately 69–71 m.y. old (see site chapters, this volume). In detail, the deeper sites are progressively slightly younger than the crestal site. Within each hole the biostratigraphy of intercalated sediments indicates episodic eruption of flows over intervals of up to a million years.

The basalts vary from aphyric to highly plagioclase phyric, as in the schematic stratigraphy in Figure 1. Samples described in this chapter were taken at the approximate (interpolated for variable recovery rate) positions indicated in Figure 1. The sample set was selected to cover the range of variability among the basalt units, using the freshest material available (surface alteration and vein material excluded). In addition, multiple sam-

pling of individual units allowed for characterization of intraunit variability due to both primary magmatic (crystal-liquid sorting) and secondary alteration processes. Except for the highly altered top 20 m of Hole 525A and aphyric basalts of Holes 528 and 527, the overall degree of alteration is slight to moderate, with the development of clay minerals in the groundmass and the occurrence of calcite (\pm pyrite) in veins. The old age and prolonged elevation have in no way predated complete, pervasive alteration.

PETROGRAPHY

In Hole 525A on the crest of the Walvis Ridge the recovered 103-m section of the basement complex comprises a sequence of basalt flows and pillows, with minor intercalated volcanoclastic sediments. Five separate extrusive units are recognizable (Fig. 1), one of which is a distinct 20-m-thick pillow basalt sequence

MINERAL CHEMISTRY

with numerous fresh glass selvages. The petrography of these aphyric basalts is reasonably uniform. Groundmasses consist predominantly of subophitic intergrowths of plagioclase (50–60%) and augite (45–35%). Subordinate titanomagnetite (2–10%) occurs as both a primary and a secondary (alteration) groundmass phase. Occasional lone plagioclase phenocrysts are observable in the drill core. Glass is present in the groundmass matrix of fine-grained basalt in the upper part of Unit 5 and dominates in glassy pillow margins of Unit 4, where it has an orange brown, nonpleochroic coloration. Recognizable glassy chilled margins in the other two holes are completely altered.

In Hole 528, midway up the western flank of the Ridge, the 80-m basement complex section recovered is composed of basalt flows separated by interlayered biogenic and volcanoclastic sediments. The seven cooling units distinguished are of two types (Fig. 1). The first consists of massive, highly plagioclase phyric basalt, the second of vesicular aphyric to sparsely plagioclase phyric basalt. Plagioclase phenocrysts in the former range up to 10×15 mm in size, 25 vol.% in abundance, and are complexly twinned and zoned. Sparse olivine and clinopyroxene phenocrysts also occur therein, but the olivine is altered to clays. Groundmass textures in both types are subophitic.

In Hole 527, the deepest on the Walvis Ridge transect, the 44-m basement complex section recovered is again composed of massive basalt flows with minor interlayered sediments. Of five distinguishable cooling units, the top four are sparsely plagioclase-olivine (altered)-augite to highly plagioclase phyric with subophitic groundmass textures. The highly plagioclase phyric basalt is petrographically similar to that which occurs at Site 528. The 20+ -m-thick basal unit is aphyric and varies in texture from subophitic to intergranular to "pegmatitic," indicative of local internal differentiation during crystallization.

Further petrographic detail and thin section descriptions for individual basalt samples may be found in the Sites 525, 528, and 527 chapters (this volume).

ANALYTICAL TECHNIQUES

Whole-rock sample preparation comprised sawn surface removal by abrasion with silicon carbide, ultrasonic cleaning in acetone and distilled water, coarse crushing in a steel jaw crusher, and grinding in agate vessels. Small ultrapure separates of fresh isotropic glass from one pillow margin and plagioclase from one highly plagioclase phyric basalt were prepared by hand-picking.

Powders were analyzed for major and selected trace elements, using X-ray fluorescence (XRF) spectrometric techniques described in Willis et al. (1971). Estimates of precision and detection limits applicable to the XRF data reported here are listed in le Roex et al. (1981). In addition, Rb, Sr, K, Cs, Sm, and Nd concentrations were measured on a subset of powders and on two grain separates by isotope dilution. Chemical separation and mass spectrometric techniques for determination of Rb, Sr, K, and Cs concentrations and $^{87}\text{Sr}/^{86}\text{Sr}$ ratios are as described in Hart and Brooks (1977); for Sm and Nd concentrations and $^{143}\text{Nd}/^{144}\text{Nd}$ ratios as adapted from the technique of Richard et al. (1976) and summarized in Zindler et al. (1979). Acid leaching of basalt samples to remove alteration phases was not attempted because the poor selectivity of this technique makes it appropriate only to rocks of close to zero isotopic age correction. The procedure followed for electron microprobe (EMP) analysis of mineral phases is summarized in le Roex et al. (1981).

A brief reconnaissance study of the clinopyroxene and plagioclase chemistry of selected Holes 525A, 528, and 527 basalts revealed little variation within basalt types. The results are summarized in Figures 2 and 3 (point analyses) and Tables 1 and 2 (averages for different morphologies in individual samples).

All groundmass clinopyroxene compositions are augitic with an average of $\text{Wo}_{42}\text{En}_{43}\text{Fs}_{15}$ and Fe enrichment no higher than Fs_{20} (Fig. 2). No phenocryst augite was analyzed but it is likely of very similar composition. Phenocryst plagioclase is extremely calcic (An_{85-90}) with relatively narrow margins showing strong normal zoning down to An_{60-70} (Table 2; Fig. 3). Groundmass plagioclase ranges from An_{68} to as low as An_{40} . The average groundmass plagioclase is approximately An_{60} , which is not substantially different from phenocryst rim compositions.

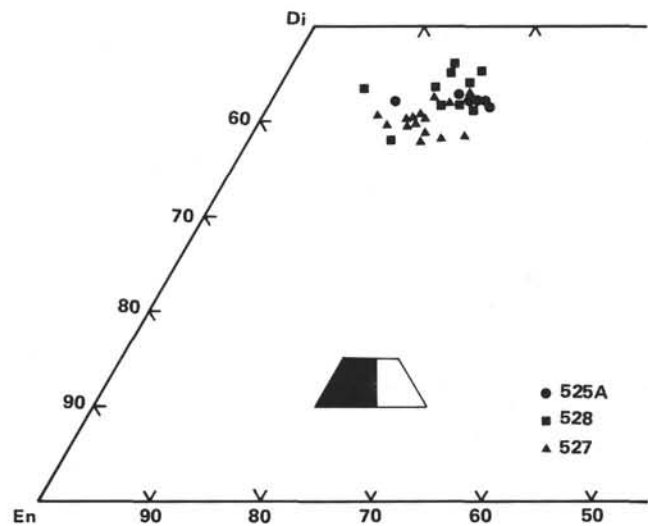


Figure 2. Clinopyroxene compositions (point analyses) in basalts from Holes 525A, 528, and 527 on the Walvis Ridge transect.

Table 1. Averaged EMP compositions of clinopyroxene (and one glass matrix) in basalts from Holes 525A, 527, and 528 on the Leg 74 Walvis Ridge transect.

	Sample (interval in cm)								
	525A 56-5, 94-98 gdm.	525A 62-1, 10-15 μ phen.	525A 62-1, 10-15 glass	528 42-1, 50-53 gdm.	528 42-3, 8-11 gdm.	527 39-4, 35-39 gdm.	527 40-1, 53-55 gdm.	527 40-2, 36-39 gdm.	527 44-1, 49-52 gdm.
SiO_2	49.29	47.82	53.02	50.09	48.00	50.51	51.66	50.23	49.65
TiO_2	1.33	1.95	2.73	0.90	1.65	0.81	0.52	0.76	1.03
Al_2O_3	3.03	4.49	14.45	3.72	4.88	3.27	1.97	3.83	2.88
Cr_2O_3	0.04	0.12	—	—	—	0.12	0.11	0.14	—
FeO	10.68	10.94	11.62	9.19	9.34	9.42	8.77	9.13	9.69
MnO	0.26	0.24	0.19	0.25	0.23	0.24	0.23	0.22	0.22
MgO	14.18	13.64	3.85	15.24	13.67	15.80	16.41	15.83	14.81
CaO	20.23	20.09	7.76	20.31	21.60	18.90	19.61	18.86	20.67
Na_2O	0.43	0.46	3.64	0.24	0.34	0.31	0.22	0.31	0.35
K_2O	—	—	1.82	—	—	—	—	—	—
Total	99.47	99.75	99.08	99.93	99.71	99.38	99.49	99.31	99.29
Wo	41.9	42.2	—	41.7	45.1	39.2	39.8	39.3	42.4
En	40.8	39.9	—	43.5	39.7	45.6	46.3	45.8	42.1
Fs	17.3	17.9	—	14.8	15.2	15.2	13.9	14.9	15.5

Note: gdm = groundmass, μ phen = microphenocryst.

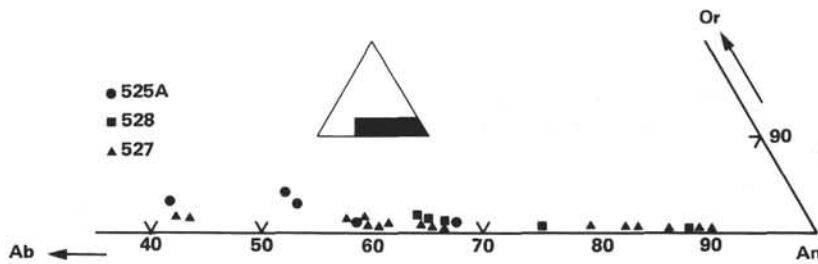


Figure 3. Plagioclase compositions (point analyses) in basalts from Holes 525A, 528, and 527 on the Walvis Ridge transect.

WHOLE-ROCK CHEMISTRY

The major element compositions of the basalts from Holes 525A, 528 and 527 are listed in Table 3 and illustrated in variation diagrams in Figure 4. For graphical representation, compositions have been normalized to 100% volatile-free with all Fe expressed as FeO (designated FeO*). Fields in Figure 4 enclose samples from the same cooling unit to show the direction and relative magnitude of intraunit variation. The latter is generally

small fraction of the total variation among units. In order of increasing relative variation, major element abundances range from 49–53% for SiO₂, 14–20% for Al₂O₃, 9–13% for FeO*, 2.4–3.6% for Na₂O, 4–7% for MgO, 6–13% for CaO, 1–3% for TiO₂, 0.1–0.5% for P₂O₅, and 0.2–2.4% for K₂O. Overall, positive correlations exist between SiO₂, TiO₂, P₂O₅, and K₂O (Fig. 4). The last three elements are incompatible (largely excluded from phenocryst olivine, clinopyroxene, and calcic plagioclase) so that the correlations are suggestive of fractionation

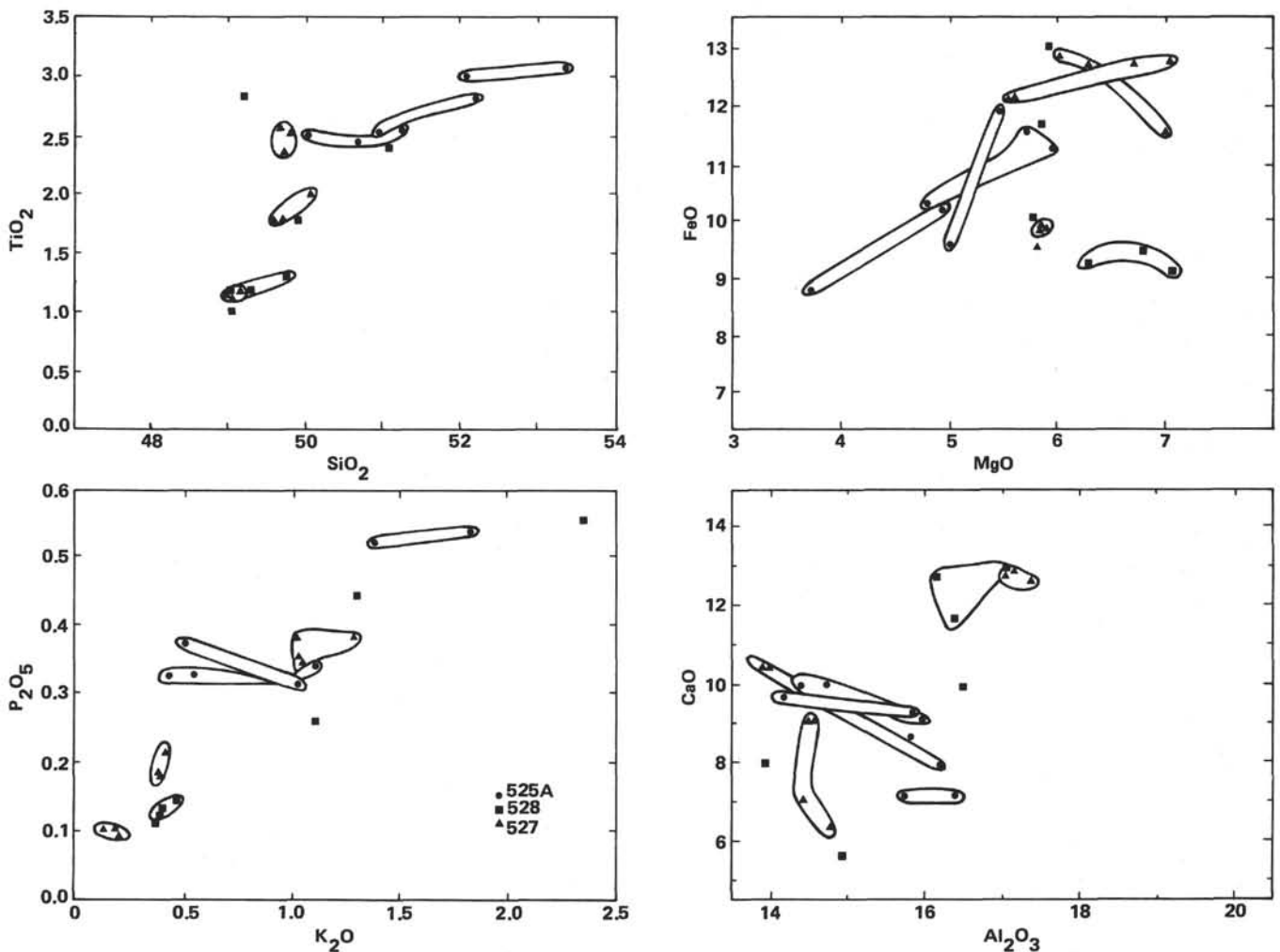


Figure 4. Major element variation diagrams for basalts from Holes 525A, 528, and 527 on the Walvis Ridge transect. Sample compositions were normalized to 100 wt.% volatile-free with all Fe as FeO (designated FeO*). Fields enclose samples from the same cooling unit.

Table 2. Averaged EMP compositions of plagioclase in basalts from Holes 525A, 527, and 528 on the Leg 74 Walvis Ridge transect.

	Sample (interval in cm)												
	525A		528		527		527		527		527		
	56-5, 94-98	62-1, 10-15	42-1, 50-53	42-3, 8-11	39-4, 35-39	40-1, 53-55	40-2, 36-39	44-1, 49-52					
	gdm.	μ phen.	gdm.	phen.		gdm.	phen.	gdm.	phen.		gdm.	gdm.	
				core	rim			core	rim				
SiO ₂	53.57	55.02	52.43	46.41	50.80	51.41	46.19	55.22	52.00	47.46	51.51	51.08	53.31
Al ₂ O ₃	28.18	27.23	29.19	33.36	29.95	29.18	34.31	27.81	29.32	34.20	31.39	30.46	28.86
FeO	0.65	0.87	0.67	0.37	0.71	0.92	0.10	0.19	0.82	0.08	0.16	123	0.71
MgO	0.16	0.17	0.13	0.26	0.22	0.36	0.34	0.17	0.23	0.24	0.25	0.37	0.10
CaO	11.71	10.73	13.21	18.13	14.57	14.03	17.70	10.71	12.69	15.79	12.76	13.25	12.11
Na ₂ O	5.08	5.30	4.04	1.32	3.41	3.89	1.22	5.49	4.55	1.74	3.64	4.01	4.73
K ₂ O	0.34	0.65	0.31	—	0.12	0.16	—	0.17	0.14	—	0.08	0.10	0.26
Total	99.69	99.95	99.98	99.85	99.78	99.95	99.86	99.75	99.75	99.51	99.78	99.50	100.08
An	55.0	50.9	63.2	88.4	69.7	66.0	88.9	51.5	60.5	83.4	65.6	64.2	57.7
Ab	43.2	45.4	35.0	11.6	29.6	33.1	11.1	47.6	38.8	16.6	33.9	35.2	40.9
Or	1.8	3.7	1.8	—	0.7	0.9	—	0.9	0.7	—	0.5	0.6	1.4

Note: gdm. = groundmass, μ phen. = microphenocryst, phen. = phenocryst.

relationships among samples. In the plot of P₂O₅ versus K₂O, loss of K₂O (probably due to alteration) is suggested for several samples from the crestal Hole 525A by virtue of their lateral displacement to lower K₂O values. For Al₂O₃, CaO, MgO, and FeO* (major components of phenocryst plagioclase, clinopyroxene, and olivine) no clear overall trends are apparent. Small-scale variation within individual cooling units is probably attributable to crystal-liquid sorting, but this remains to be quantitatively evaluated.

C.I.P.W. norms have been calculated for all compositions after assigning a blanket Fe₂O₃/FeO wt. ratio of 0.2 and normalizing to 100% volatile-free. Basalts from the crestal Hole 525A are all quartz tholeiites (13–18% normative hypersthene; 1–4% normative quartz). Basalts from the two flank sites are all olivine tholeiites (5–23% normative hypersthene; 3–11% normative olivine). The normative data support the more evolved nature of the Hole 525A basalts as shown in Figure 4.

Concentrations of trace elements Rb, Ba, Sr, Zr, Nb, Cr, V, Sc, Ni, Co, Zn, Cu, S, and Y are listed in Table 3 along with Zr/Nb, Ba/Nb, Zr/Y, and K/Rb ratios. In addition, concentrations of Cs, Nd, and Sm for a subset of samples appear in Tables 4 and 5.

Concentrations of the incompatible elements are in general higher than those observed for typical MORB (Erlank and Reid, 1974; Erlank and Kable, 1976), although large ranges in concentration have been demonstrated both for MORB (e.g., le Roex and Dick, 1981) and for the samples reported in this study. This is the case for each of the three sites, and such in-site variation can probably be attributed to crystal fractionation effects, as has been demonstrated at other localities (le Roex and Dick, 1981; le Roex et al., 1981). Variations in concentration for Zr, Nb, and Ba are shown in Figure 5 (Zr-Nb) and Figure 6 (Ba-Nb). Zr and Nb are known to be resistant to seawater alteration (Hart et al., 1974), and, in view of the consistency of Ba/Nb ratios (Table 3), this also appears to be the case for Ba in the samples analyzed. Nb and Ba are the most incompatible of the elements reported here and show ranges in concentration from 6–53 ppm and 72–626 ppm, respectively; the range observed for Zr is slightly less (62–360 ppm).

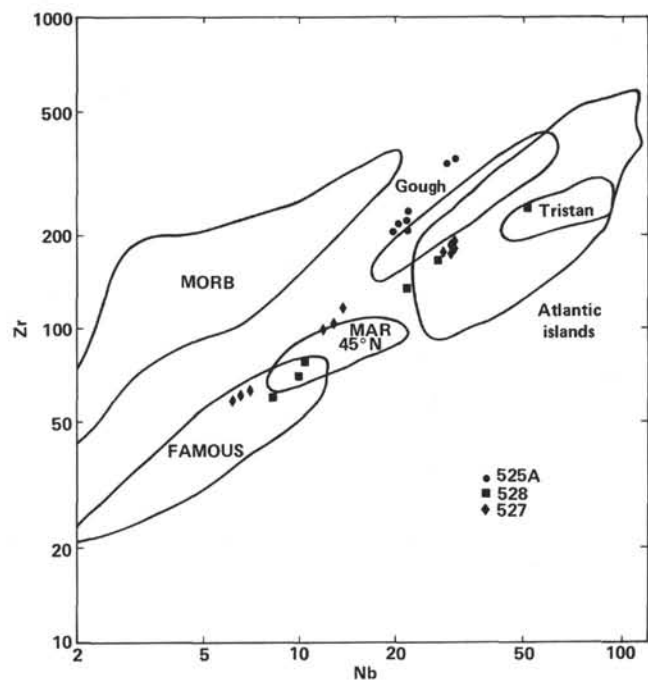


Figure 5. Variation between Zr and Nb contents (ppm, log scale) of basalts from Holes 525A, 528, and 527 on the Walvis Ridge transect and comparison with other seafloor and ocean island basalts. All data have been obtained by XRF in the Dept. of Geochemistry, University of Cape Town. Data sources: MORB (N-type), Kable (1972), Erlank and Reid (1974), le Roex and Dick (1981); MORB (E-type), FAMOUS area, le Roex et al. (1981) and Mid-Atlantic Ridge at 45°N, Erlank and Kable (1976); Atlantic islands, Kable (1972). Only the fields for data from Gough and Tristan da Cunha are shown. Other Atlantic islands include Ascension, Azores Group, Bouvet, Fogo, Iceland (various), Jan Mayen, Madeira, Saint Helena and Tenerife. All samples contain <55% SiO₂.

Speculation that the basalts from the three sites may be related in part by crystal fractionation is not supported by interelement ratios such as Zr/Nb and Zr/Y (Table 3), which indicate that the Hole 525A basalts form a separate group. A plot of Zr/Nb versus Zr/Y (not shown) indicates that the Hole 525A samples are displaced as a group from the Holes 528 and 527 samples. Our present knowledge of the partitioning behavior of

Table 3. Major and trace element compositions of basalts from Holes 525A, 528, and 527 on the Leg 74 Walvis Ridge transect.

	Sample (interval in cm)										
	525A 56-5, 90-94	525A 57-1, 119-124	525A 57-5, 20-25	525A 59-1, 91-95	525A 59-4, 35-39	525A 63-1, 86-91	525A 63-2, 63-68	528 39-1, 131-136	528 40-2, 112-117	528 40-3, 70-76	528 42-1, 40-45
SiO ₂	49.53	48.80	49.55	50.31	50.20	52.37	51.10	48.80	48.24	47.96	48.18
TiO ₂	2.39	2.45	2.47	2.71	2.48	3.01	2.93	1.27	1.16	1.14	2.27
Al ₂ O ₃	14.02	14.34	15.48	15.23	13.95	16.04	15.46	16.04	15.83	16.66	14.08
Fe ₂ O ₃	12.17	12.47	10.97	10.14	12.92	9.53	11.01	9.83	10.26	10.00	12.17
MnO	0.12	0.12	0.10	0.09	0.19	0.11	0.10	0.15	0.15	0.15	0.18
MgO	5.88	5.65	4.66	4.89	5.33	3.74	4.91	7.00	6.70	6.20	5.57
CaO	9.75	9.78	8.80	8.86	9.49	7.02	7.00	11.42	12.40	12.49	5.32
Na ₂ O	2.84	2.93	3.19	3.16	2.49	3.85	3.55	2.80	2.46	2.47	3.62
K ₂ O	0.56	0.46	1.10	0.52	1.03	1.81	1.38	0.48	0.41	0.41	2.21
P ₂ O ₅	0.32	0.31	0.33	0.36	0.31	0.52	0.50	0.14	0.12	0.13	0.52
LOI	0.85	0.91	1.75	1.91	0.90	0.67	1.14	0.97	0.91	0.93	1.74
H ₂ O-	1.68	1.88	1.50	2.04	0.51	0.98	1.22	1.86	1.58	1.35	3.38
Total	100.11	100.10	99.90	100.22	99.82	99.67	100.30	100.76	100.22	99.89	99.24
Rb	3.4	2.2	16	3.3	18	13	7.3	9.3	6.1	7.9	38
Ba	342	343	344	280	276	505	528	153	138	136	626
Sr	419	429	432	443	360	481	480	251	232	241	285
Zr	210	217	229	245	225	359	346	81	72	72	250
Nb	20	22	22	22	21	31	30	11	10	9.8	53
Cr	31	34	58	42	45	41	37	48	83	63	5.0
V	289	301	309	356	323	314	299	287	255	247	301
Sc	31	33	39	40	37	31	31	39	39	35	22
Ni	26	28	36	37	30	40	27	50	64	54	10
Co	43	44	49	44	47	54	39	49	48	46	36
Zn	88	105	94	105	115	111	93	69	61	63	98
Cu	51	54	51	67	65	32	36	166	135	134	27
S	306	313	356	891	1570	268	283	1130	1425	1395	1350
Y	29	32	31	40	36	39	41	23	24	22	45
Zr/Nb	11	10	10	11	11	12	11	7.7	7.0	7.3	4.8
Ba/Nb	17	16	16	13	13	16	18	15	14	14	12
Zr/Y	7.2	6.8	7.4	6.1	6.3	9.2	8.4	3.5	3.0	3.3	5.6
K/Rb	1410	1770	590	1360	490	1220	1610	430	580	440	520

Note: Major (wt.%) and trace (ppm) element concentrations determined by XRF techniques described in Willis et al. (1971). Estimated precision and detection limits are listed in le Roex et al. (1981).

Zr, Nb, and Y during crystal fractionation processes (le Roex et al., 1981) does not support the derivation of the more evolved Hole 525A basalts from the Holes 528 and 527 basalts by such processes.

Further evaluation of Figures 5 and 6 indicates the enriched nature of the Walvis Ridge transect samples. All these samples have Zr/Nb ratios which are lower than normal, depleted, or N-type MORB but which are similar to samples from the Mid-Atlantic Ridge at 45°N and from the FAMOUS area, taken to be representative of enriched or E-type MORB (Erlank and Kable, 1976; Wood, 1979). The Walvis samples also have Zr/Nb ratios similar to those found in Atlantic island basalts, but in view of the range of Zr/Nb encountered in the Walvis samples no clear association with any single island can be postulated for all the samples. The Hole 525A samples do have similar Zr/Nb ratios to those from Gough Island, but none of the samples have ratios as low as those observed in Tristan da Cunha.

A plot of Zr-Ba (not shown) reveals that Ba, like Nb, is also enriched relative to Zr in the Walvis samples. However, Figure 6 indicates that Ba is even more enriched than Nb, such that Ba/Nb ratios are higher than those observed for both N- and E-type MORB. Furthermore, the Walvis samples also have Ba/Nb ratios higher

than those observed in most Atlantic island basalts but which are, however, within the range reported for Gough and Tristan da Cunha. This enrichment of Ba is perhaps the most striking feature of the trace element geochemistry of the Walvis samples and to our knowledge has not been demonstrated for other seafloor basalts apart from where alteration has been involved (as indicated earlier, the consistency of the Ba/Nb ratios in the Walvis samples argues against introduction of Ba by seawater alteration).

Other relatively incompatible elements are variably well correlated. In correlations with Zr, Nb, or Ba, the overall degree of scatter (due to alteration) is low for Nd, Sm, and Sr; intermediate for P, Y, and Zn; high for K, Rb, and Cs; and extreme for S. Alteration-induced changes in original Nd and Sm abundances appear to be minimal and these abundances can be used to infer rare earth patterns. Nd ranges from 15 to 73 and Sm from 14 to 48 times the average of chondrite abundances (Nakamura, 1974). Light rare earth enrichment increases dramatically from the highly plagioclase phyric basalts to the aphyric basalts.

The effects of alteration can be assessed by inspection of K-Rb-Cs relationships. In Figure 7 K/Rb ratios range from 410 to 1770. Substantial variation in K/Rb

Table 3. (Continued).

Sample (interval in cm)													
528 42-2, 145-150	528 44-3, 126-131	528 47-3, 23-28	527 39-1, 40-45	527 39-3, 114-119	527 40-1, 106-111	527 40-2, 56-62	527 41-1, 64-70	527 41-4, 10-15	527 42-4, 99-104	527 43-1, 71-76	527 44-1, 52-57	527 44-4, 100-105	
48.02	47.83	48.59	48.86	48.95	49.20	48.84	48.93	48.82	47.76	48.56	48.95	48.86	
0.99	1.72	2.80	1.97	1.76	1.76	1.14	1.11	1.17	2.45	2.45	2.33	2.33	
19.69	15.78	13.73	15.86	13.70	13.80	17.28	17.07	16.91	14.17	14.06	14.30	14.28	
7.83	10.61	14.18	12.34	13.94	13.94	10.89	10.85	10.79	13.55	13.72	13.17	13.16	
0.11	0.21	0.24	0.11	0.18	0.18	0.16	0.17	0.16	0.21	0.20	0.18	0.18	
5.10	5.61	5.94	6.93	6.04	6.30	5.89	5.93	5.86	6.86	6.59	5.53	5.56	
13.04	9.54	7.85	7.78	10.26	10.30	12.50	12.77	12.66	6.12	6.90	8.93	8.93	
2.43	3.04	3.56	3.10	2.98	2.93	2.41	2.40	2.52	3.22	3.46	3.57	3.42	
0.39	1.09	1.31	0.43	0.41	0.41	0.24	0.22	0.17	1.26	1.02	1.05	1.06	
0.11	0.25	0.43	0.21	0.18	0.18	0.09	0.10	0.10	0.37	0.37	0.35	0.34	
0.92	1.45	0.95	1.16	0.41	0.32	0.48	0.27	0.19	1.36	1.05	0.52	0.64	
1.52	2.42	1.10	1.69	1.34	1.20	0.77	0.63	0.93	2.32	1.94	1.75	1.76	
100.15	99.55	100.68	100.44	100.15	100.52	100.69	100.46	100.28	99.65	100.33	100.63	100.52	
6.0	17	20	6.3	7.2	6.9	4.8	2.9	1.6	19	13	20	16	
110	291	451	155	151	147	81	72	74	361	354	358	333	
224	282	305	175	146	144	139	140	143	276	283	311	300	
62	139	171	121	107	104	61	62	64	179	176	191	184	
8.3	22	28	14	13	12	6.2	6.7	7.0	29	30	31	30	
96	36	21	83	69	78	70	80	71	13	12	15	20	
238	311	427	474	397	404	281	270	285	362	363	207	354	
32	34	28	54	42	42	37	38	38	36	38	31	35	
62	42	18	61	52	57	49	52	51	17	17	20	26	
41	45	42	57	50	50	44	43	45	42	43	44	45	
59	84	110	107	108	98	73	69	67	96	85	97	101	
117	118	57	220	202	200	150	147	152	76	65	79	92	
627	711	2385	1400	1845	1820	1305	1320	1345	1985	1955	1965	449	
22	33	44	38	40	39	26	26	28	39	40	40	42	
7.4	6.3	6.2	8.4	8.4	8.0	9.8	9.2	9.1	6.1	5.9	6.2	6.1	
13	13	16	11	12	12	13	11	11	12	12	12	11	
2.8	4.2	3.9	3.2	2.7	2.7	2.3	2.4	2.3	4.6	4.4	4.8	4.4	
560	570	560	590	490	500	410	620	880	560	660	440	560	

Table 4. K, Rb, and Cs concentrations (ppm) in basalts from Holes 525A, 528, and 527 on the Leg 74 Walvis Ridge transect.

Sample (interval in cm)	K	Rb	Cs	K/Rb	K/Cs ($\times 10^{-3}$)
Hole 525A					
57-1, 119-124	3915	2.29	0.030	1710	131
59-4, 35-39	8698	18.3	0.25	475	35
59-4, 35-39	8986	18.8	0.17	478	53
63-1, 86-91	15680	12.5	0.032	1250	490
63-2, 63-68	12010	7.22	0.036	1660	334
Hole 528					
42-1, 40-45	19240	38.1	0.082	505	235
42-2, 145-150	3348	6.03	0.029	555	115
47-3, 23-28	11140	19.9	0.054	560	206
Hole 527					
41-4, 10-15	1475	1.72	0.029	858	51
44-1, 52-57	9436	19.2	0.039	491	242

within individual units from Hole 525A is evident. The samples with high K/Rb are the same samples that appear to have lost K (Fig. 4). This in turn suggests that they sustained even greater relative losses of Rb. Conversely, at least one of the 525A samples with low K/Rb

has retained close to magmatic K and Rb contents. The fresh glass separate has marginally higher K and Rb contents and a K/Rb ratio essentially identical to the corresponding whole-rock sample (Table 4). K/Cs ratios (Table 4, Fig. 7) show even greater scatter than K/Rb, with an order of magnitude variation from 35,000 to 490,000. K, Rb, and Cs appear to have been variably mobile, in keeping with the conclusions of Hart (1969, 1971), but nevertheless appear to be enriched in the Walvis samples when compared with either N- or E-type MORB.

The overall relative variation for the compatible elements in Table 3 is large but erratic for Ni, Cr, and Cu and subdued for Sc, Co, and V. The evolved nature of all the Walvis samples is shown by their low Ni and Cr contents (10-64 ppm Ni; 5-96 ppm Cr) compared with values of 120 ppm Ni and 296 ppm Cr for "average" MORB (Erlank and Reid, 1974) and 270 ppm Ni and 580 ppm Cr for primitive olivine-basalts from the FA-MOUS area (le Roex et al., 1981). This strongly indicates olivine and chromite fractionation in the magmas that gave rise to the recovered Walvis samples. The abundances of the other compatible elements are within the ranges reported in the literature for MORB and do not warrant further comment.

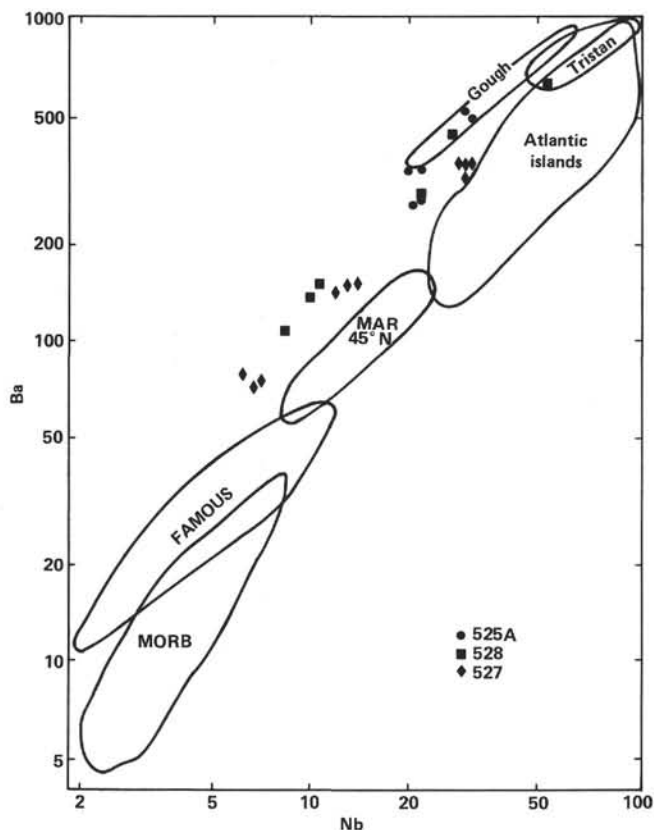


Figure 6. Variation between Ba and Nb contents (ppm, log scale) of basalts from Holes 525A, 528, and 527 on the Walvis Ridge transect and comparison with other seafloor and ocean island basalts. Sources of data are as in Figure 5 with the exception of le Roex and Dick (1981), as the Ba data from this source are believed to be affected by seawater alteration.

Nd AND Sr ISOTOPE VARIATION

Combined Nd and Sr isotope ratios and Sm, Nd, Rb, and Sr concentrations measured on single dissolutions of representative whole rocks and the glass and plagioclase separates are listed in Table 5. Whole rock samples are from separate cooling units, except for the pair of samples from Unit 5 in Hole 525A. Initial ratios have been calculated for an average age of 70 m.y. (see Geological Setting and Sampling). Present-day and initial ratios are plotted on a Nd-Sr isotope correlation diagram in Figure 8 along with fields of published data for MORB and several ocean islands. Vectors joining initial and present-day ratios indicate isotopic evolution in these basalts over the 70 m.y. since their formation. Except for the basalts with high Rb/Sr ratios (e.g., Sample 528-42-1, 40–45 cm), the isotopic evolution of their sources over the equivalent short time period will not have been substantially different.

Values for the fresh glass separate and the corresponding whole rock (Sample 525A-59-4, 35–39 cm) are also plotted in Figure 8. Their $^{147}\text{Sm}/^{144}\text{Nd}$, $^{143}\text{Nd}/^{144}\text{Nd}$, and $^{87}\text{Rb}/^{86}\text{Sr}$ ratios are essentially identical. However, their $^{87}\text{Sr}/^{86}\text{Sr}$ ratios (present or initial) differ by 2 parts in 10^4 . This serves to illustrate the extent of alteration of some whole-rock $^{87}\text{Sr}/^{86}\text{Sr}$ ratios. A fur-

ther possible indication of this is the $^{87}\text{Sr}/^{86}\text{Sr}$ ratio obtained for the plagioclase separate from a highly plagioclase phyric basalt (Sample 527-41-4, 10–15 cm). Because of its low $^{87}\text{Rb}/^{86}\text{Sr}$ ratio, the plagioclase present-day $^{87}\text{Sr}/^{86}\text{Sr}$ ratio is essentially equal to the initial ratio. This differs from the whole-rock $^{87}\text{Sr}/^{86}\text{Sr}$ initial ratio by 4 parts in 10^4 . The set of basalts in Table 5 was chosen to represent the maximum range in major and trace element chemistry identified in Table 3 and thus includes, for example, the aphyric basalts in Sample 528-42-1, 40 cm and 528-47-3, 23 cm, which are petrographically moderately altered. Assuming unchanged $^{143}\text{Nd}/^{144}\text{Nd}$ ratios, these appear to have suffered the largest alteration-induced increases in $^{87}\text{Sr}/^{86}\text{Sr}$ relative to the overall trend.

Systematic negative covariation of $^{143}\text{Nd}/^{144}\text{Nd}$ and $^{87}\text{Sr}/^{86}\text{Sr}$ ratios is apparent in Figure 8 notwithstanding second-order alteration effects. Basalts from the Ridge crest Hole 525A individually and collectively have the lowest $^{143}\text{Nd}/^{144}\text{Nd}$ (0.51238) and highest $^{87}\text{Sr}/^{86}\text{Sr}$ (0.70512) ratios. Highly plagioclase phyric basalts from the midflank Hole 528 and lower flank Hole 527 have the highest $^{143}\text{Nd}/^{144}\text{Nd}$ (0.51270) and the lowest $^{87}\text{Sr}/^{86}\text{Sr}$ (0.70417) ratios. Aphyric basalts from both flank sites have isotope ratios that are intermediate between these extremes.

Whole-rock $^{143}\text{Nd}/^{144}\text{Nd}$ and $^{87}\text{Sr}/^{86}\text{Sr}$ ratios are, respectively, negatively and positively correlated with Nd (9–46 ppm) and Sr (146–495 ppm) concentrations. This is shown graphically in Figure 9, in which initial ratios are plotted against reciprocal concentrations. The order of samples in the crude trends outlined is essentially the same for Sr and Nd and corresponds to that of the isotope ratio correlation. Basalts from the Ridge crest Hole 525A thus have the highest Nd and Sr concentrations, whereas the highly plagioclase phyric basalts from the flank Holes 528 and 527 have the lowest. Differentiation and dilution effected by crystal-liquid sorting would have changed reciprocal concentration values and contributed to scatter in Figure 9. Further scatter in the Sr plot in Figure 9 is attributable to alteration-induced increases in $^{87}\text{Sr}/^{86}\text{Sr}$ ratio discussed in the foregoing.

A crude positive correlation also exists between initial $^{143}\text{Nd}/^{144}\text{Nd}$ ratio and Sm/Nd ratio (Fig. 10). This translates into decreasing $^{143}\text{Nd}/^{144}\text{Nd}$ ratio with increasing degree of light rare earth enrichment in basalts of the same age. Rb/Sr ratios are so scattered (combined effects of alteration and differentiation) as to obscure any possible original positive correlation between $^{87}\text{Sr}/^{86}\text{Sr}$ and $^{87}\text{Rb}/^{86}\text{Sr}$ ratios (Fig. 10).

DISCUSSION

The quartz tholeiitic basalts from Hole 525A on the Walvis Ridge crest represent the trace element and isotopic extreme of magmas erupted to form this 70 m.y. old segment of the ridge. Although their major element chemistry is indistinguishable from the more evolved examples of mid-ocean ridge tholeiites (MORB) encountered on East Pacific spreading centers (Clague and Bunch, 1976), their incompatible trace element and isotopic characteristics are unparalleled among ocean floor

Table 5. Rb, Sr, Sm, and Nd concentrations^a and Sr and Nd isotopic compositions of basalts from Holes 525A, 528, and 527 on the Leg 74 Walvis Ridge transect.

Sample (interval in cm)	Rb	Sr	⁸⁷ Rb/ ⁸⁶ Sr	⁸⁷ Sr/ ⁸⁶ Sr _p ^b	⁸⁷ Sr/ ⁸⁶ Sr _i ^c	Sm	Nd	¹⁴⁷ Sm/ ¹⁴⁴ Nd	¹⁴³ Nd/ ¹⁴⁴ Nd _p ^b	¹⁴³ Nd/ ¹⁴⁴ Nd _i ^c
Hole 525A										
57-1, 119-124	2.29	437	0.0152	0.70498 ± 5	0.70496	6.74	29.8	0.1367	0.512461 ± 21	0.512398
59-4, 35-39	18.3	367	0.1443	0.70500 ± 5	0.70486	7.03	31.1	0.1369	0.512466 ± 23	0.512403
59-4, 35-39	18.8	375	0.1451	0.70486 ± 3	0.70472	7.29	32.5	0.1356	0.512456 ± 17	0.512394
63-1, 86-91	12.5	488	0.0742	0.70512 ± 3	0.70505	9.53	44.9	0.1283	0.512376 ± 17	0.512317
63-2, 63-68	7.22	495	0.0422	0.70511 ± 3	0.70507	9.65	45.7	0.1277	0.512379 ± 16	0.512321
Hole 528										
42-1, 40-45	38.1	293	0.3764	0.70498 ± 2	0.70461	6.80	33.8	0.1217	0.512555 ± 17	0.512499
42-2, 145-150	6.03	224	0.0779	0.70423 ± 3	0.70415	2.50	9.23	0.1637	0.512699 ± 35	0.512624
47-3, 23-28	19.9	310	0.1858	0.70444 ± 3	0.70426	5.65	24.1	0.1420	0.512682 ± 22	0.512617
Hole 527										
41-4, 10-15	1.72	146	0.0341	0.70417 ± 3	0.70414	2.80	9.40	0.1800	0.512694 ± 13	0.512612
41-4, 10-15	0.067	180	0.0011	0.70385 ± 3	0.70385	0.0539	0.176	0.1848		
44-1, 52-57	19.2	313	0.1776	0.70455 ± 3	0.70437	6.40	28.3	0.1376	0.512566 ± 16	0.512503

Note: Plag. = plagioclase.

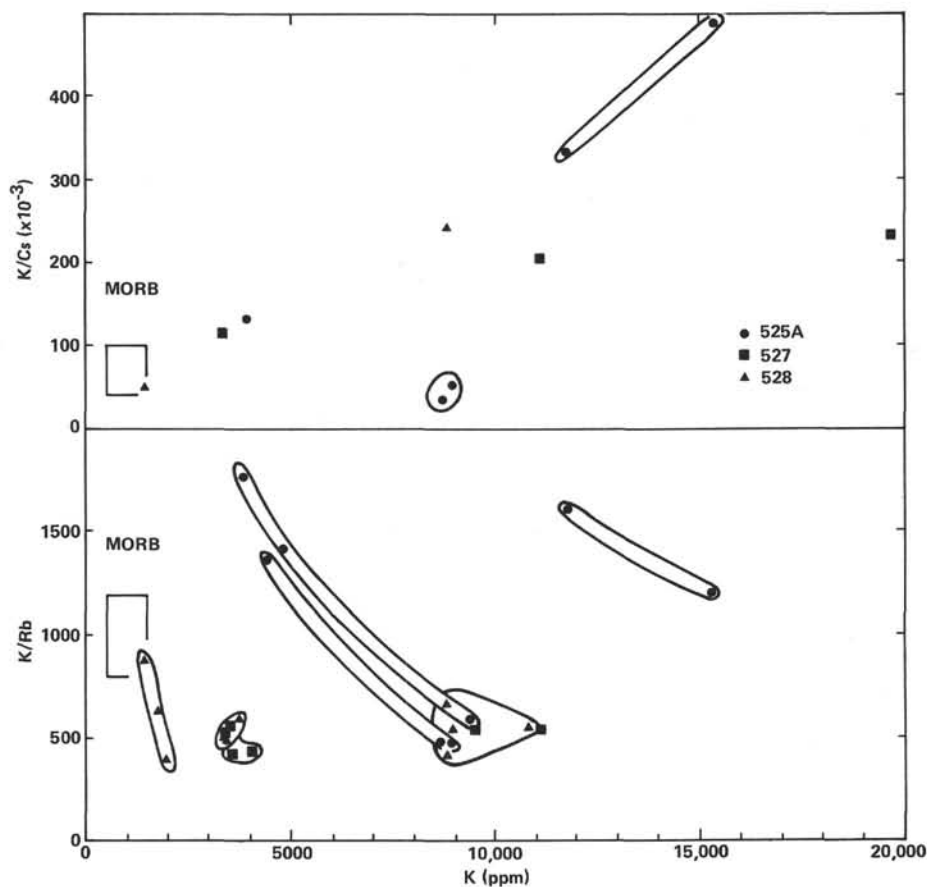
^a Concentrations (ppm) by isotope dilution, with precision for Sr, Nd, and Sm ~ 0.3% and for Rb ~ 1%.^b Errors are 2σ_{mean} on in-run statistics, multiplied by 10⁵ for Sr and 10⁶ for Nd. ⁸⁷Sr/⁸⁶Sr values are normalized to 0.70800 for E and A SrCO₃. ¹⁴³Nd/¹⁴⁴Nd values are normalized to ¹⁴⁶Nd/¹⁴⁴Nd = 0.7219 and ¹⁴³Nd/¹⁴⁴Nd = 0.512640 for BCR-1.^c Initial ratios calculated for an age of 70 m.y., using λ_{Rb} = 1.42 × 10⁻¹¹ y.⁻¹ and λ_{Sm} = 6.54 × 10⁻¹² y.⁻¹.

Figure 7. Variation between K/Rb and K/Cs ratios and K contents (ppm) of basalts from Holes 525A, 528, and 527 on the Walvis Ridge transect. Fields enclose samples from the same cooling unit. Typical MORB compositions are from Hart (1976).

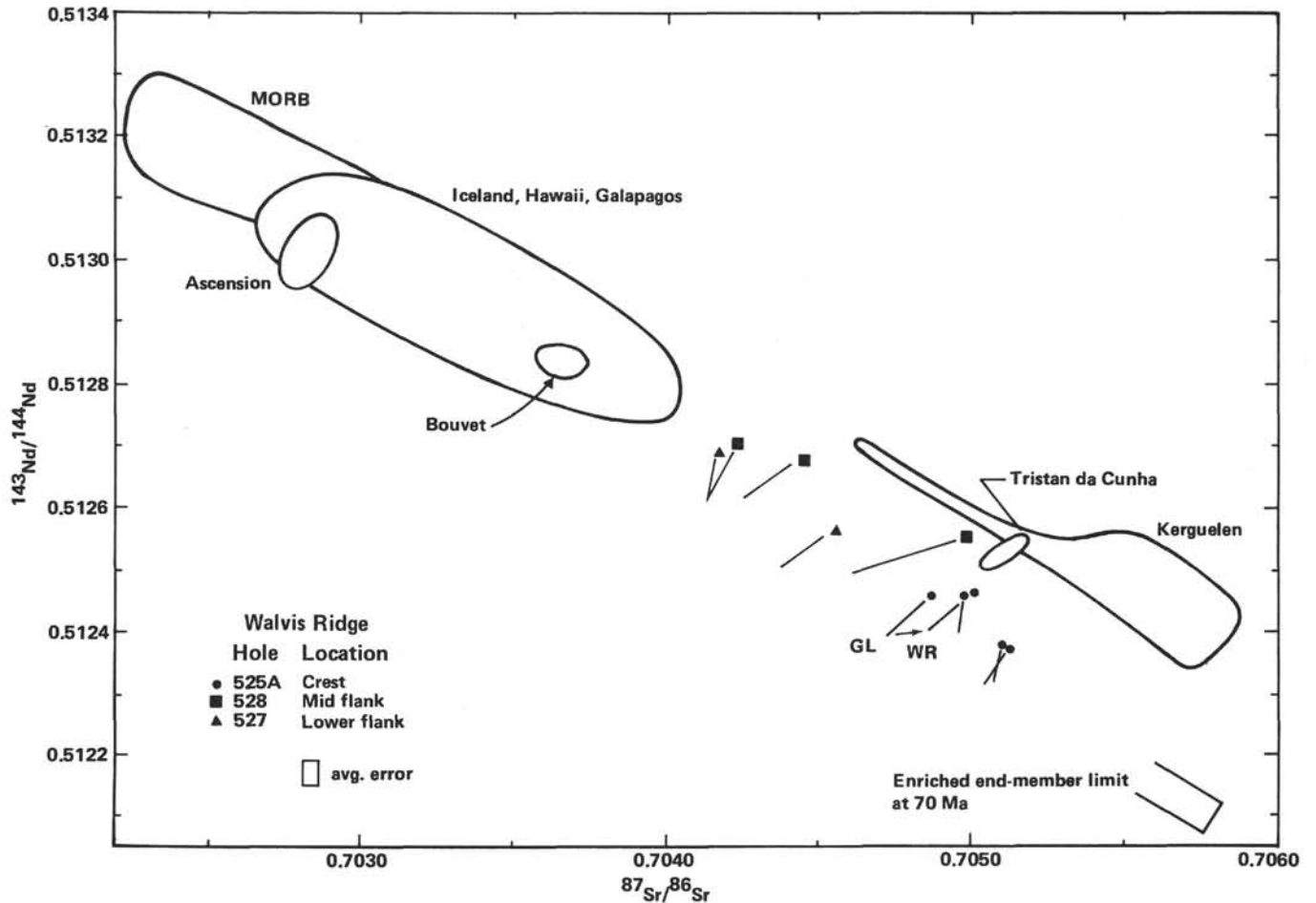


Figure 8. Nd-Sr isotope correlation diagram showing the Walvis Ridge basalt trend parallel to an extension of the oceanic mantle array defined by fields for MORB and some recent ocean island volcanics. Aphyric basalts from the Ridge crest lie at the lower right end of this trend and highly phyrific basalts from the flank at its upper left end. Lines indicate isotopic evolution of individual basalts over the 70 m.y. since formation of this segment of the ridge. Whole-rock initial $^{87}\text{Sr}/^{86}\text{Sr}$ ratios suffered variable increases because of exchange with seawater, as exemplified by the vector between those of a fresh glass and corresponding whole rock (Sample 525A-59-4, 35-39 cm). The enriched end-member limit derived by interpretation of the initial ratio-reciprocal concentration trends as mixing lines (Fig. 9) is shown at lower right. Data sources: Richard et al., 1976 (MORB, Iceland); De Paolo and Wasserburg, 1976b (MORB, Hawaii); O'Nions et al., 1977 (MORB, Hawaii, Iceland, Ascension, Bouvet, Tristan da Cunha); White and Hofmann, 1978 (Galapagos); Dosso and Murthy, 1980 (Kerguelen). All Nd data normalized to $^{146}\text{Nd}/^{144}\text{Nd} = 0.7219$ (O'Nions et al., 1977) and $^{143}\text{Nd}/^{144}\text{Nd} = 0.51264$ for BCR-1 (Dosso and Murthy, 1980).

tholeiites. The closest analogues are the tholeiitic basalts of the Ninety East Ridge in the Indian Ocean (Hekinian, 1974), which have similar Sr isotopic characteristics (Whitford and Duncan, 1978). Olivine tholeiitic basalts from Holes 528 and 527 on the mid- and lower flank of the Walvis Ridge have trace element and isotopic characteristics intermediate between those of the crestal basalts and typical or N-type MORB which might constitute the floor of the Angola and Cape Basins north and south of the ridge.

The changes in K, Rb, Cs, and S abundances and increases in $^{87}\text{Sr}/^{86}\text{Sr}$ ratio suggested in previous sections are almost certainly due to exchange with seawater (Hart, 1969, 1971; Hart et al., 1974). Such exchange leaves the Zr and Nb abundances and Nd isotopic composition of submarine basalts essentially unchanged (e.g., Hart et al., 1974; O'Nions et al., 1978). Alteration of submarine basalts with substantial sediment cover is restricted to a short period (<5-10 m.y.) after eruption (Hart and Staudigel, 1978; Richardson et al., 1980;

Staudigel et al., 1981). The $^{87}\text{Sr}/^{86}\text{Sr}$ ratio of 70-m.y.-old seawater would have been approximately 0.7078 (cf. Hart and Staudigel, 1978, and references therein). Exchange between seawater (~8 ppm Sr) and Walvis Ridge basalts (146-495 ppm Sr) would therefore produce mild increases in the whole-rock $^{87}\text{Sr}/^{86}\text{Sr}$ ratio. Changes in Rb/Sr ratio were dominated by losses and gains in Rb. Calculated initial $^{87}\text{Sr}/^{86}\text{Sr}$ ratios are maximum values for magmatic initial ratios. Nevertheless, alteration effects have not obscured the clear overall correlation between Sr and Nd isotope ratios.

Together the freshest basalts from the three Walvis Ridge sites define an essentially linear trend on a Nd-Sr correlation diagram (Fig. 8). This parallels an extension of the mantle array (De Paolo and Wasserburg, 1979; Allegre et al., 1979) outlined by the data for MORB and some recent ocean island volcanics (Richard et al., 1976; De Paolo and Wasserburg, 1976b; O'Nions et al., 1977). Basalts from the crest of the Walvis Ridge lie at the low $^{143}\text{Nd}/^{144}\text{Nd}$, high $^{87}\text{Sr}/^{86}\text{Sr}$ end of this trend slightly but

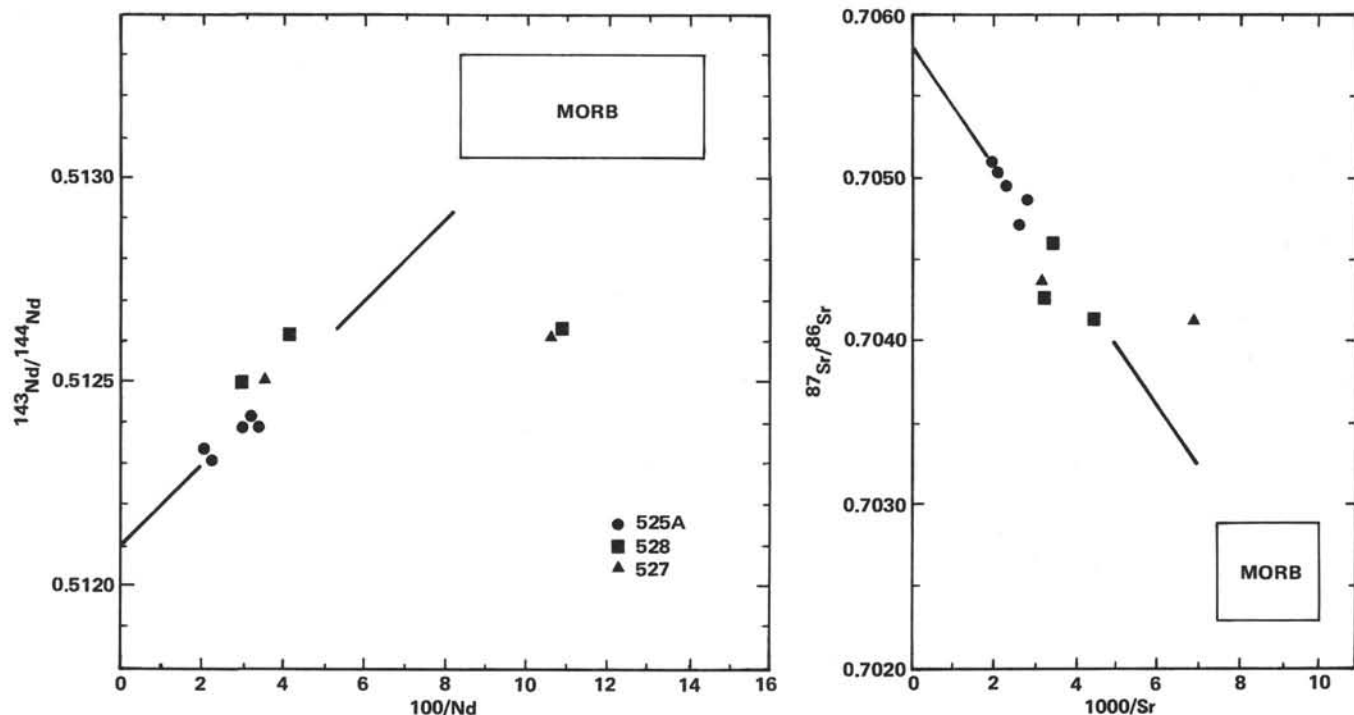


Figure 9. Variation between initial isotope ratio (70 m.y.) and reciprocal concentration for basalts from Holes 525A, 528, and 527 on the Walvis Ridge transect. As discussed in the text, Nd and Sr concentrations have been variously affected by differentiation and dilution due to crystal-liquid sorting, whereas initial $^{87}\text{Sr}/^{86}\text{Sr}$ ratios have been variously increased by exchange with seawater. Lines show extrapolations to intercepts of 0.5121 at $1/\text{Nd} = 0$ and 0.7058 at $1/\text{Sr} = 0$ (infinite enrichment) in one direction and typical MORB compositions in the other. If these are interpreted as simple binary mixing lines, the intercept composition represents the limit of the enriched end-member. This composition also falls on an extension of the Nd-Sr array in Figure 8. MORB data sources: Schilling, 1971; Hart, 1976; and references in Figure 8.

distinctly lower $^{87}\text{Sr}/^{86}\text{Sr}$ ratios (for equivalent $^{143}\text{Nd}/^{144}\text{Nd}$ ratio) than alkaline basalts on the spatially associated island of Tristan da Cunha (O'Nions et al., 1977) and on Kerguelen Island in the Indian Ocean (Dosso and Murthy, 1980). At the current level of sampling, basalts and related differentiates from Tristan and other South Atlantic islands close to the MAR (Ascension, Bouvet) appear to have restricted ranges in Sr and Nd isotopic composition (O'Nions and Pankhurst, 1974; O'Nions et al., 1977). The isotope ratios of basalts from the Walvis Ridge flank trend away from those at its crest in the direction of those for Bouvet, Ascension, and MORB (Fig. 8).

Three classes of models for the origin of the Walvis Ridge basalts derive from consideration of their distinct geochemical characteristics. Because of variation in isotopic and incompatible interelement ratios, derivation of different magma types cannot be modeled simply by crystal-liquid sorting (differentiation/dilution) of compositionally equivalent magmas or by partial melting of a homogeneous source. Plausible models which might account for the isotopic and incompatible trace element variations include (1) crustal contamination of melts from a homogeneous mantle, (2) mixing of melts from heterogeneous mantle, and (3) melting of mantle with small-scale heterogeneity. These three models and their applicability to the Walvis Ridge basalts are discussed in the following.

Crustal Contamination of Melts from a Homogeneous Mantle

Mantle-derived magmas of the Walvis Ridge could potentially undergo contamination by oceanic crust, continental crust, or marine sediments. If the original "primitive" magmas of the Walvis Ridge had MORB characteristics, contamination by preexisting (Mesozoic) hydrothermally altered oceanic crust might cause small increases in $^{87}\text{Sr}/^{86}\text{Sr}$. However, such contamination would leave $^{143}\text{Nd}/^{144}\text{Nd}$ and the Zr and Nb abundances essentially unchanged and is therefore not a viable mechanism to account for the geochemical characteristics of Walvis Ridge basalts.

Contamination by continental crust could produce the low $^{143}\text{Nd}/^{144}\text{Nd}$ ratios, high $^{87}\text{Sr}/^{86}\text{Sr}$ ratios and high Ba contents observed in the Walvis Ridge basalts, given the widespread occurrence of these characteristics in old continental crustal materials (e.g., Carter et al., 1978; DePaolo and Wasserburg, 1979). However, magneto- and biostratigraphic age constraints and the character of recovered samples (see site chapters, this volume) argue against Walvis Ridge segments originating as blocks of continental crust as suggested by van der Linden (1980).

Contamination by marine sediments could account for the high Ba and Nb abundances in Walvis Ridge basalts but fails to explain the other incompatible element

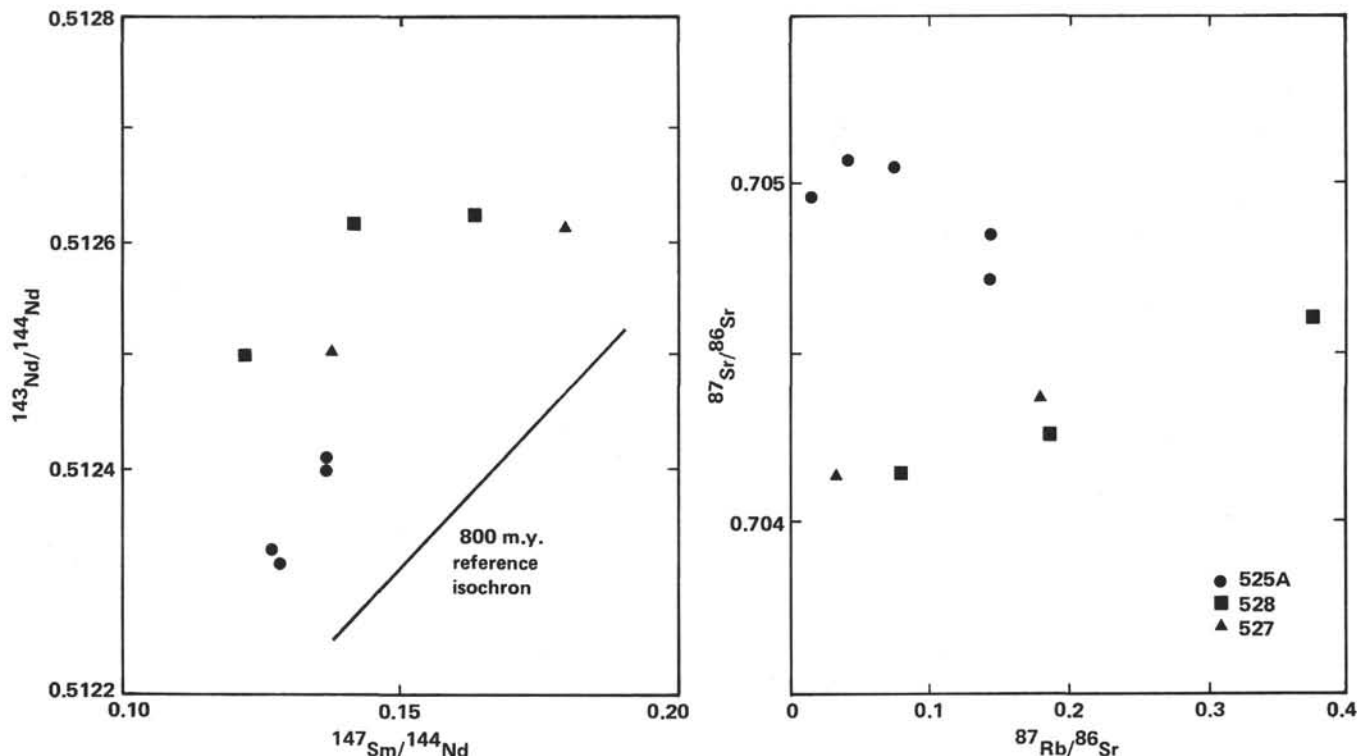


Figure 10. Sm-Nd and Rb-Sr isochron diagrams showing variation between initial isotope ratio (70 m.y.) and parent-daughter ratio. As discussed in the text, ratios have been variously affected by differentiation and alteration. An 800 m.y. Sm-Nd isochron is shown for reference.

and isotopic ratio correlations. Sediments with a significant terrigenous (continental) component which might be more suitable contaminants have not been recorded in the holes comprising the Walvis Ridge transect.

Mixing of Melts from Heterogeneous Mantle

Binary mixing of end-member magmas is the simplest model requiring a heterogeneous mantle. This is equivalent to the "LOM" mantle model (large-scale, old heterogeneity; mixing of melts) suggested by Zindler et al. (1979) as the preferred explanation for the trace element and isotopic characteristics of the Reykjanes Peninsula basalts of Iceland. Adaptation of this model to the Walvis Ridge basalts would predict an approximately linear array on an Nd-Sr isotope diagram because differences in Nd and Sr concentrations for the two end-members would not be large enough to induce obvious curvature (Langmuir et al., 1978). Approximate limits for the end-member compositions in such a mixing system can be derived from plots of initial isotopic composition versus reciprocal concentration (Fig. 9). An $^{143}\text{Nd}/^{144}\text{Nd}$ ratio of 0.5121 and an $^{87}\text{Sr}/^{86}\text{Sr}$ ratio of 0.7058 can be obtained for the most "enriched" end-member by extrapolation of the rather crude trends shown in Figure 9, which are variously affected by fractionation and alteration, to $1/\text{Nd} = 0$ and $1/\text{Sr} = 0$ (infinite enrichment). With increasing reciprocal concentration (depletion), the trends in Figure 9 extrapolate in the general direction of MORB, but it is not possible to uniquely define a "depleted" end-member.

In such a binary mixing model, correlations between isotope ratio and parent-daughter ratio (Fig. 10) would

be mixing lines and would not have any age significance except in the case of a simple two-source model in which both sources differentiated from a common parent at a discrete time. For this case the mixing lines would correspond to two-point isochrons. As noted in Figure 10, correlations between isotope ratio and parent-daughter ratio are poorly developed. This is especially so for the Rb-Sr system, where seawater alteration has undoubtedly been active.

The inferred minimum $^{143}\text{Nd}/^{144}\text{Nd}$ ratio of the enriched end-member (0.5121) and even the observed minimum $^{143}\text{Nd}/^{144}\text{Nd}$ ratio of the Ridge crest basalts (0.51238) are distinctly lower than the value adopted for "bulk earth" ("chondritic uniform reservoir," DePaolo and Wasserburg, 1976a), even considering the uncertainty which must be attached to any such estimate (Jacobsen and Wasserburg, 1980). This implies that the source of at least one component in the petrogenetic scheme for the Walvis Ridge basalts underwent an ancient increase in Nd/Sm and Rb/Sr above bulk earth values in contrast to the decrease in these ratios shown by MORB-type mantle sources.

A simple binary mixing model, as suggested by the isotope data, necessarily requires that all other combinations of elements and ratios also form mixing lines. The interelement relationships shown in Figure 11 effectively preclude any significant participation by N-type MORB as the depleted end-member in a magma mixing model, and the high Ba contents of the Walvis Ridge basalts (Fig. 6) appear to eliminate the possibility of E-type MORB being an end-member in a two-component model. Finally, the combined distribution of Zr/Nb and

Zr/Y ratios (Table 3) in the Ridge flank basalts ($Zr/Nb = 5-10$; $Zr/Y = 5-2$) relative to those in the more evolved Ridge crest basalts ($Zr/Nb = 10-12$; $Zr/Y = 6-9$) apparently rules out any mixing model which is restricted to two components, even when allowance is made for fractionation of interelement ratios by magmatic differentiation.

Melting of Mantle with Small Scale Heterogeneity

An alternative model requiring a heterogeneous mantle involves the partial melting of a chemically modified mantle which has been variably "enriched," such that the Ridge crest basalts from Hole 525A are representative of those portions of the mantle which show the greatest degree of enrichment. A simple example of such a model is the "SOS" mantle model (small-scale, old heterogeneity; solid state, mixing of sources) of Zindler et al. (1979). Volcanic products derived from a composite source in which the enriched and depleted portions had the same initial isotopic compositions describe the same correlations of isotope ratio with reciprocal concentration and parent-daughter ratio as in the LOM

model described in the previous section. In the SOS model, however, the latter correlations are more likely to have real age significance. In the ideal case where basalt parent-daughter ratios reflect those of their sources, the age of the enrichment event can be obtained. The poorly developed positive correlation between initial $^{143}\text{Nd}/^{144}\text{Nd}$ and $^{147}\text{Sm}/^{144}\text{Nd}$ ratios for Walvis Ridge basalts (Fig. 10) is not well enough defined to yield a meaningful age directly. However, given that relative decreases in Sm/Nd ratios caused by differentiation are likely to be greater for the more "evolved" Ridge crest basalts from Hole 525A than for the Ridge flank basalts, then a minimum age of approximately 800 (+70) m.y. can be obtained for the postulated mantle enrichment event. Clearly, if this event involved components with different initial isotopic compositions or was not discrete (i.e., >2-stage model), its timing is necessarily obscure and the age obtained has no significance.

Although the presence of compositionally different mantle beneath the Walvis Ridge is supported by its anomalous Rayleigh wave dispersion characteristics (Chave, 1979), the precise nature of a possible enrich-

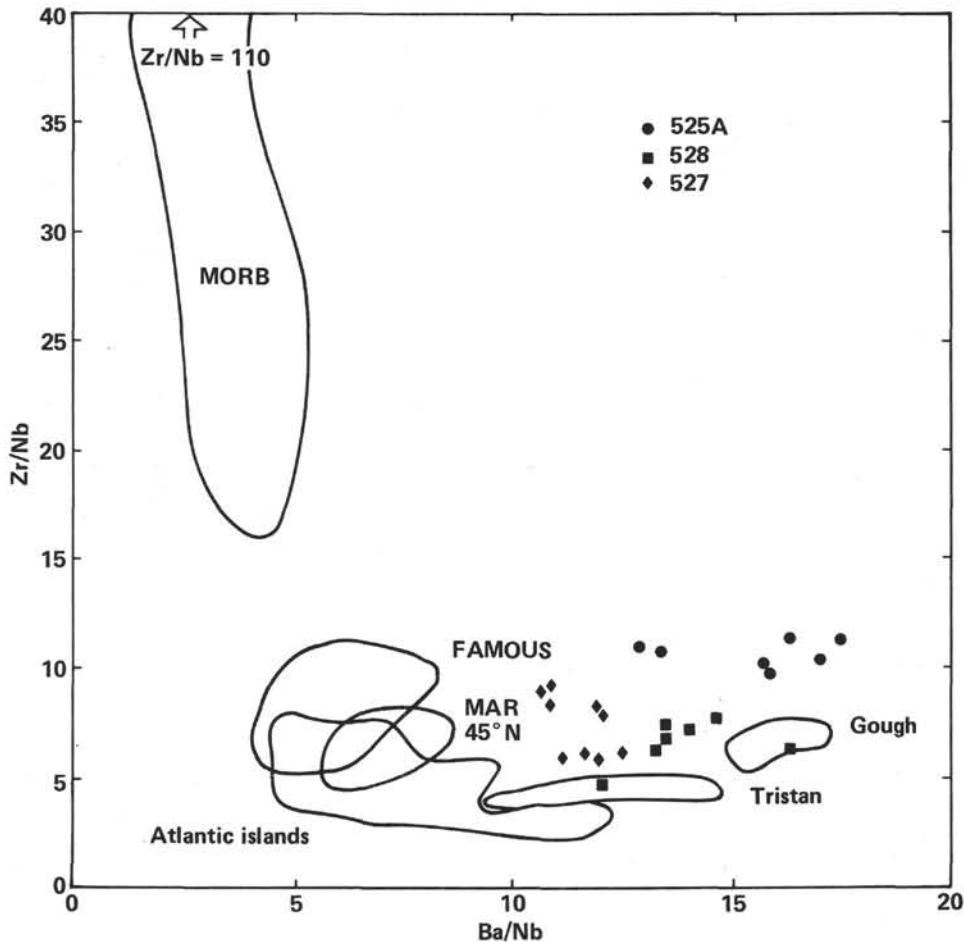


Figure 11. Variation between Zr/Nb and Ba/Nb ratios of basalts from Holes 525A, 528, and 527 on the Walvis Ridge transect and comparison with other seafloor and ocean island basalts. Note that any simple two-component mixing should produce a straight line on this diagram between potential end-members (effects of magmatic fractionation on these ratios are considered to be negligible). Sources of data are as in Figure 6.

ment event cannot be defined at this state. Nevertheless, it is appropriate to discuss briefly the following options for mantle enrichment mechanisms and events below the Walvis Ridge:

1) Invasion of a homogeneous mantle source by small volume enriched melts which crystallize as veins of enriched material and which do not subsequently equilibrate isotopically with the host mantle wall rock. Such melts could be derived in two ways: (1) by direct melting of mantle (e.g., Hanson, 1977; Wood, 1979; Zindler et al., 1979). In the simplest case the small volume melts are derived from material of the same composition as that which they invade, and this is equivalent to the SOS model previously discussed. (2) By subduction induced melting as a consequence of recycling of subducted crust (e.g., O'Nions et al., 1979; Allegre et al., 1980; Hoffmann and White, 1980). This could also effectively be a contamination model if the subducted material contributes directly to the small volume melts. In the simplest case this contribution does not occur, and the subduction process acts merely as a triggering mechanism, in which case the melting process is effectively the same as the SOS model.

For the simple cases outlined in (1) and (2), the previously noted minimum enrichment age of 800–900 m.y. can be viewed in the context of the geodynamic history of the regional lithosphere prior to opening of the South Atlantic. The Walvis Ridge meets the southern African continental margin in the vicinity of the SW–NE-trending Damaran orogen of Pan-African age. With regard to (1) it is pertinent that the earliest Damaran volcanic activity (Naauwpoort volcanics and Matchless amphibolites) has also been dated as approximately 800 m.y. old (Hawkesworth et al., 1981). The Matchless amphibolites have higher Sm/Nd and $^{143}\text{Nd}/^{144}\text{Nd}$ ratios than the bulk earth value at the time of their emplacement—i.e., ratios consistent with derivation from an N-type MORB source when age differences are allowed for (Hawkesworth et al., 1981). In the context of (2) McWilliams and Kroner (1981) have recently proposed a model involving rifting, heating, and stretching of the lithosphere beneath the Damara Belt. In this complex, broadly defined model, *intracrustal* subduction is also suggested, and any one of these processes could result in the generation and migration of melt in the mantle.

Although the correlation of mantle enrichment beneath the present Walvis Ridge with Damaran orogenesis cannot be considered as more than a suggestion at this stage, the tremendous surface expression of the Damaran episode should perhaps be viewed as a consequence of mantle processes. Clearly, clarification of the mantle enrichment age discussed in the foregoing is required.

2) Invasion of a homogeneous mantle source by metasomatic fluids which crystallize partly as veins and partly (as a consequence of reequilibration) as replacement products of preexisting minerals in the host mantle. The overall process is one of infiltration metasomatism. Although this process is similar to that involving the introduction of small volume melts, we prefer to make a distinction between them, since it is likely that

the chemical character of the metasomatic fluids will be different from that of the melts. This may be particularly important for volatile and incompatible elements, although it is not currently possible to quantify such differences.

The mineralogical and chemical evidence for metasomatism of mantle-derived nodules has been documented by Lloyd and Bailey (1975), Harte et al., (1975), and Erlank and Rickard (1977). Sr isotopic evidence for a suite of K-richterite-bearing peridotites from one southern African kimberlite (Bultfontein) suggests a minimum age of approximately 150 m.y. for the metasomatic event (Erlank and Shimizu, 1977; Erlank et al., 1980), which was tentatively linked with the cessation of Karoo volcanicity. This particular metasomatic event would appear to be too young for the postulated enrichment event in the mantle underlying the Walvis Ridge. However, Nd and Sr isotopic measurements on diopside separates from garnet-phlogopite lherzolites (which lack K-richterite) from the Bultfontein kimberlite are indicative of an older enrichment event in this part of the mantle (Menzies and Murthy, 1980). It is noteworthy that these diopsides have $^{143}\text{Nd}/^{144}\text{Nd}$ ratios as low as 0.51185 and $^{87}\text{Sr}/^{86}\text{Sr}$ ratios as high as 0.7072. Kimberlite nodules clearly contain evidence of the existence of metasomatized mantle which could potentially give rise to the Walvis Ridge basalts. However, progress has yet to be made in understanding the cause and timing of the metasomatic event(s) and the identity and source of the metasomatizing fluids.

As noted in the previous section, any petrogenetic model for the Walvis Ridge basalts must provide more than two compositional components, although only two isotopic components are required. In this respect the two models of small-scale heterogeneity in the mantle discussed earlier suffer the same defect as the LOM model discussed in the previous section. However, there are two plausible ways to incorporate an extra component into the small-scale heterogeneity models: (1) The small volume melts or metasomatic fluids could be introduced into a mantle that is already heterogeneous as the result of some previous event. (2) Both small volume melts and metasomatic fluids (of different composition) are introduced into homogeneous mantle, either simultaneously or sequentially.

We find the latter possibility appealing since it seems highly probable that introduction of a metasomatic fluid could well trigger small volume partial melting as a consequence of depressing the mantle solidus. In either case it would appear that the SOS model is capable of satisfying the existing constraints which are imposed on the petrogenesis of the Walvis Ridge basalts by isotopic data and incompatible element interrelationships.

CONCLUSIONS

The upper 100 m of basement in a NNW–SSE-trending block of the Walvis Ridge consist of submarine tholeiitic basalts (with intercalated sediments) erupted approximately 70 Ma, an age equivalent to that of immediately adjacent oceanic crust in the Angola Basin. This is consistent with formation at the paleo mid-ocean ridge.

The Nd and Sr isotopic compositions of Ridge crest basalts indicate that their mantle source region contains an old component which is Nd/Sm- and Rb/Sr-enriched. The isotopic signature of the Walvis Ridge basalts is similar to that of alkaline basalts on the spatially associated island of Tristan da Cunha, but with distinctly lower values of $^{143}\text{Nd}/^{144}\text{Nd}$. The incompatible element concentrations are similar to those in oceanic islands or E-type MORB, but detailed examination of Zr-Ba-Nb-Y interelement relationships shows that they are not consistent with any simple two-component model of magma mixing or partial melting. They also exclude major involvement of depleted (N-type) MORB material or its mantle sources in the petrogenesis of Walvis Ridge basalts. In our preferred petrogenetic model, the Walvis Ridge basalts were derived by partial melting of mantle similar to an E-type MORB source which had become heterogeneous on a small scale owing to the introduction of small volume melts and metasomatic fluids. The relatively low Ni and Cr contents of the Walvis Ridge basalts indicate that they further evolved by fractional crystallization prior to eruption.

ACKNOWLEDGMENTS

Compliments are due to Captain Clark and the gang aboard the *Glomar Challenger* for a classic cruise. P. Richard and C. Allegre are acknowledged for help and advice in setting up Paris-style Nd chemistry at M.I.T. We thank M. Brauteseth, K. Burrhus, D. Hall, K. Thurmond, and T. Miele for shore-based technical and professional assistance. Reviews by S. R. Hart and A. P. le Roex are appreciated. Support from the Harry Crossley Foundation (SHR), the University of Cape Town, the CSIR, and NSF grant #7803342-EAR (to S. R. Hart) is acknowledged.

REFERENCES

- Allegre, C. J., Ben Othman, D., Polve, M., and Richard, P., 1979. The Nd-Sr isotopic correlation in mantle materials and geodynamic consequences. *Phys. Earth Planet. Inter.*, 19:293-306.
- Allegre, C. J., Brevart, O., Dupre, B., and Minster, J.-F., 1980. Isotopic and chemical effects produced in a continuously differentiating convecting Earth mantle. *Phil. Trans. R. Soc. London*, A 297:447-477.
- Burke, K. C., and Wilson, J. T., 1976. Hot spots on the Earth's surface. *Sci. Am.*, 235:46-57.
- Carter, S. R., Evensen, N. M., Hamilton, P. J., and O'Nions, R. K., 1978. Neodymium and strontium isotope evidence for crustal contamination of continental volcanics. *Science*, 202:743-747.
- Chave, A. D., 1979. Lithospheric structure of the Walvis Ridge from Rayleigh wave dispersion. *J. Geophys. Res.*, 84:6840-6848.
- Clague, D. A., and Bunch, T. E., 1976. Formation of ferrobasalt at East Pacific midocean spreading centers. *J. Geophys. Res.*, 81:4247-4256.
- DePaolo, D. J., and Wasserburg, G. J., 1976a. Nd isotopic variations and petrogenetic models. *Geophys. Res. Lett.*, 3:249-252.
- , 1976b. Inferences about magma sources and mantle structure from variations of $^{143}\text{Nd}/^{144}\text{Nd}$. *Geophys. Res. Lett.*, 3:743-746.
- , 1979. Petrogenetic mixing models and Nd-Sr isotopic patterns. *Geochim. Cosmochim. Acta*, 43:615-627.
- Detrick, R. S., and Watts, A. B., 1979. An analysis of isostasy in the world's oceans: Part 3—Aseismic ridges. *J. Geophys. Res.*, 84:3637-3653.
- Dingle, R. V., and Simpson, E. S. W., 1976. The Walvis Ridge: a review. In Drake, C. L. (Ed.), *Geodynamics: Progress and Prospects*: Washington (AGU), 160-176.
- Dosso, L., and Murthy, V. R., 1980. A Nd isotopic study of the Kerguelen Islands: inferences on enriched oceanic mantle sources. *Earth Planet. Sci. Lett.*, 48:268-276.
- Erlank, A. J., Allsopp, H. L., Duncan, A. R., and Bristow, J. W., 1980. Mantle heterogeneity beneath southern Africa: evidence from the volcanic record. *Phil. Trans. R. Soc. London*, A 297:295-307.
- Erlank, A. J., and Kable, E. J. D., 1976. The significance of incompatible elements in mid-Atlantic ridge basalts from 45°N with particular reference to Zr/Nb. *Contrib. Mineral. Petrol.*, 54:281-291.
- Erlank, A. J., and Reid, D. L., 1974. Geochemistry, mineralogy and petrology of basalts, Leg 25, DSDP. In Simpson, E. S. W., Schlich, R., et al., *Init. Repts. DSDP*, 25: Washington (U.S. Govt. Printing Office), 543-551.
- Erlank, A. J., and Rickard, R. S., 1977. Potassic richterite-bearing peridotites from kimberlite and the evidence they provide for upper mantle metasomatism. In Boyd, F. R., and Meyer, H. O. A. (Eds.), *Extended Abstracts, Second Int. Kimberlite Conference*: Santa Fe, New Mexico.
- Erlank, A. J., and Shimizu, N., 1977. Strontium and strontium isotope distributions in some kimberlite nodules and minerals. In Boyd, F. R., and Meyer, H. O. A. (Eds.), *Extended Abstracts, Second Int. Kimberlite Conference*: Santa Fe, New Mexico.
- Goslin, J., and Sibuet, J.-C., 1975. Geophysical study of the easternmost Walvis Ridge, South Atlantic: deep structure. *Geol. Soc. Am. Bull.*, 86:1713-1724.
- Hanson, G. N., 1977. Geochemical evolution of the suboceanic mantle. *J. Geol. Soc. Lond.*, 134:235-253.
- Hart, S. R., 1969. K, Rb, Cs contents and K/Rb, K/Cs ratios of fresh and altered submarine basalts. *Earth Planet. Sci. Lett.*, 6:295-303.
- , 1971. K, Rb, Cs, Sr and Ba contents and Sr isotopic ratios of ocean floor basalts. *Phil. Trans. Roy. Soc. London*, A 268:573-587.
- , 1976. LIL-element geochemistry, Leg 34 basalts. In Yeats, R. S., Hart, S. R., et al., *Init. Repts. DSDP*, 34: Washington (U.S. Govt. Printing Office), 283-288.
- Hart, S. R., and Brooks, C., 1977. Geochemistry and evolution of early Precambrian mantle. *Contrib. Mineral. Petrol.*, 61:109-128.
- Hart, S. R., Erlank, A. J., and Kable, E. J. D., 1974. Sea floor basalt alteration: some chemical and Sr isotopic effects. *Contrib. Mineral. Petrol.*, 44:219-230.
- Hart, S. R., and Staudigel, H., 1978. Oceanic crust: age of hydrothermal alteration. *Geophys. Res. Lett.*, 5:1009-1012.
- Harte, B., Cox, K. G., and Gurney, J. J., 1975. Petrography and geological history of upper mantle xenoliths from the Matsoku Kimberlite pipe. *Phys. Chem. Earth*, 9:477-506.
- Hawkesworth, C. J., Kramers, J. D., and Miller, R. McG., 1981. Old model Nd ages in Namibian Pan-African rocks. *Nature*, 289:278-282.
- Hekinian, R., 1972. Volcanics from the Walvis Ridge. *Nature*, 239:91-93.
- , 1974. Petrology of the Ninety East Ridge (Indian Ocean) compared to other aseismic ridges. *Contrib. Mineral. Petrol.*, 43:125-147.
- Hofmann, A. W., and White, W. M., 1980. The role of subducted oceanic crust in mantle evolution. *Carnegie Inst. Washington Ybk.*, 79:477-483.
- Humphris, S. E., and Thompson, G., 1981. Petrological and geochemical studies of rocks dredged from the Walvis Ridge, South Atlantic. *EOS (Am. Geophys. Union)*, 62:424. (Abstract)
- Jacobsen, S. B., and Wasserburg, G. J., 1980. Sm-Nd isotopic evolution of chondrites. *Earth Planet. Sci. Lett.*, 50:139-155.
- Kable, E. J. D., 1972. Some aspects of the geochemistry of selected elements in basalts and associated lavas [Ph.D. dissert.] University of Cape Town.
- Langmuir, C. H., Vocke, R. D., Hanson, G. N., and Hart, S. R., 1978. A general mixing equation with applications to Icelandic basalts. *Earth Planet. Sci. Lett.*, 37:380-392.
- le Roex, A. P., and Dick, H. J. B., 1981. Petrography and geochemistry of basaltic rocks from the Conrad fracture zone on the America-Antarctica Ridge. *Earth Planet. Sci. Lett.*, 54:117-138.
- le Roex, A. P., Erlank, A. J., and Needham, H. D., 1981. Geochemical and mineralogical evidence for the occurrence of at least three distinct magma types in the Famous region. *Contrib. Mineral. Petrol.*, 77:24-37.
- Lloyd, F. E., and Bailey, D. K., 1975. Light element metasomatism of the continental mantle: The evidence and the consequences. *Phys. Chem. Earth*, 9:389-446.

- McWilliams, M. O., and Kroner, A., 1981. Paleomagnetism and tectonic evolution of the Pan-African Damara belt, southern Africa. *J. Geophys. Res.*, 86:5147-5162.
- Menzies, M., and Murthy, V. R., 1980. Enriched mantle: Nd and Sr isotopes in diopsides from kimberlite nodules. *Nature*, 283: 634-636.
- Morgan, J., 1971. Convection plumes in the lower mantle. *Nature*, 230:42.
- , 1972. Plate motions and deep mantle convection. *Geol. Soc. Am. Mem.*, 132:7-22.
- Nakamura, N., 1974. Determination of REE, Ba, Fe, Mg, Na and K in carbonaceous and ordinary chondrites. *Geochim. Cosmochim. Acta*, 38:757-775.
- O'Nions, R. K., Carter, S. R., Cohen, R. S., Evensen, N. M., and Hamilton, P. J., 1978. Pb, Nd and Sr isotopes in oceanic ferromanganese deposits and ocean floor basalts. *Nature*, 273:435-438.
- O'Nions, R. K., Evensen, N. M., and Hamilton, P. J., 1979. Geochemical modelling of mantle differentiation and crustal growth. *J. Geophys. Res.*, 84:6091-6101.
- O'Nions, R. K., Hamilton, P. J., and Evensen, N. M., 1977. Variations in $^{143}\text{Nd}/^{144}\text{Nd}$ and $^{87}\text{Sr}/^{86}\text{Sr}$ ratios in oceanic basalts. *Earth Planet. Sci. Lett.*, 34:13-22.
- O'Nions, R. K., and Pankhurst, R. J., 1974. Petrogenetic significance of isotope and trace element variations in volcanic rocks from the Mid-Atlantic. *J. Petrol.*, 15:603-634.
- Rabinowitz, P. D., and LaBrecque, J., 1979. The Mesozoic South Atlantic Ocean and evolution of its continental margins. *J. Geophys. Res.*, 84:5973-6002.
- Rabinowitz, P. D., and Simpson, E. S. W., 1979. Final Site Survey Report—Walvis Ridge sites (IPOD Site Survey Management Data Bank).
- Richard, P., Shimizu, N., and Allegre, C. J., 1976. $^{143}\text{Nd}/^{144}\text{Nd}$, a natural tracer: an application to oceanic basalts. *Earth Planet. Sci. Lett.*, 31:269-278.
- Richardson, S. H., Hart, S. R., and Staudigel, H., 1980. Vein mineral ages of old oceanic crust. *J. Geophys. Res.*, 85:7195-7200.
- Schilling, J. G., 1971. Sea-floor evolution: rare-earth evidence. *Phil. Trans. Roy. Soc. London, A* 268:663-706.
- Staudigel, H., Hart, S. R., and Richardson, S. H., 1981. Alteration of the oceanic crust: processes and timing. *Earth Planet. Sci. Lett.*, 52:311-327.
- van der Linden, W. J. M., 1980. Walvis Ridge, a piece of Africa? *Geology*, 8:417-421.
- White, W. M., and Hofmann, A. W., 1978. Geochemistry of the Galapagos Islands: implications for mantle geodynamics and evolution. *Year Book Carnegie Inst. Washington*, 77:596-606.
- Whitford, D. J., and Duncan, R. A., 1978. Origin of the Ninety East Ridge: trace element and Sr isotope evidence. *Year Book Carnegie Inst. Washington*, 77:606-613.
- Willis, J. P., Ahrens, L. H., Danchin, R. V., Erlank, A. J., Gurney, J. J., Hofmeyr, P. K., McCarthy, T. S., and Orren, M. J., 1971. Some interelement relationships between lunar rocks and fines, and stony meteorites. *Proc. Second Lunar Sci. Conf., Geochim. Cosmochim. Acta Suppl.*, 2: Cambridge (MIT Press), 1123-1138.
- Wilson, J. T., 1963. Evidence from islands on the spreading of ocean floors. *Nature*, 197:536-538.
- Wood, D. A., 1979. A variably veined sub-oceanic upper mantle: Genetic significance for mid-ocean ridge basalts from geochemical evidence. *Geology*, 7:499-503.
- Zindler, A., Hart, S. R., Frey, F. A., and Jakobsson, S. P., 1979. Nd and Sr isotope ratios and rare earth element abundances in Reykjanes Peninsula basalts: evidence for mantle heterogeneity beneath Iceland. *Earth Planet. Sci. Lett.*, 45:249-262.